

**Christian Biertümpfel,† Jérôme
 Basquin, Rainer P. Birkenbihl,§
 Dietrich Suck and Claude
 Sauter*¶**

European Molecular Biology Laboratory,
 Structural and Computational Biology
 Programme, Meyerhofstrasse 1,
 69117 Heidelberg, Germany

† Present address: Laboratory of Molecular
 Biology, NIDDK, National Institutes of Health,
 9000 Rockville Pike, Building 5, Bethesda,
 MD 20892, USA.

§ Present address: Max-Planck-Institut für
 Züchtungsforschung, Carl-von-Linné-Weg 10,
 50829 Köln, Germany.

¶ Present address: Département 'Machineries
 Traductionnelles', UPR 9002-CNRS, Institut de
 Biologie Moléculaire et Cellulaire, 15 Rue René
 Descartes, 67084 Strasbourg, France.

Correspondence e-mail:
 c.sauter@ibmc.u-strasbg.fr

Received 26 May 2005
 Accepted 9 June 2005
 Online 15 June 2005

Characterization of crystals of the Hjc resolvase from *Archaeoglobus fulgidus* grown in gel by counter-diffusion

Holliday junction-resolving enzymes are ubiquitous proteins that play a key role in DNA repair and reorganization by homologous recombination. The Holliday junction-cutting enzyme (Hjc) from the archaeon *Archaeoglobus fulgidus* is a member of this group. The first Hjc crystals were obtained by conventional sparse-matrix screening. They exhibited an unusually elongated unit cell and their X-ray characterization required special care to avoid spot overlaps along the c^* axis. The use of an arc appended to the goniometric head allowed proper orientation of plate-like crystals grown in agarose gel by counter-diffusion. Thus, complete diffraction data were collected at 2.7 Å resolution using synchrotron radiation. They belong to space group $P3_121$ or $P3_221$, with unit-cell parameters $a = b = 37.4$, $c = 271.8$ Å.

1. Introduction

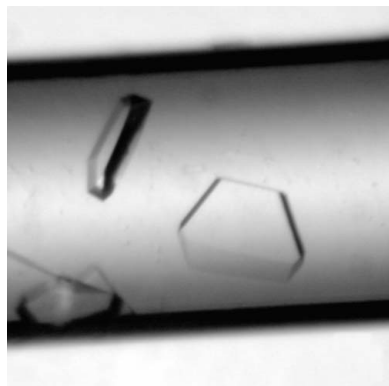
Holliday junctions (or four-way junctions) are formed during repair or reorganization of DNA by homologous recombination. They constitute mobile joints between two homologous DNA duplexes and generate new segments of heteroduplex DNA by branch-migration (Holliday, 1964). A crucial step in this process is the final exact resolution of the junction without loss of nucleotides in order to avoid any alteration of genetic information in the next cycle of replication. This step is catalyzed by Holliday junction-resolving enzymes (X-resolvases), a family of dimeric proteins that recognize DNA four-way junctions and resolve them with an extreme accuracy by introducing symmetrical nicks on both sides of the branch point (White *et al.*, 1997; Lilley & White, 2001; Sharples, 2001). X-resolvases share two common features: a catalytic activity dependent on divalent cations and a basic stretch on their surface for DNA binding.

Holliday junction-cutting enzymes (Hjc) have recently been identified in archaea (Fig. 1) and represent a conserved type of X-resolvases with similarity to type II restriction endonucleases (Komori *et al.*, 1999; Daiyasu *et al.*, 2000; Kvaratskhelia *et al.*, 2000; Neef *et al.*, 2002). Two structures of Hjc from *Sulfolobus solfataricus* and *Pyrococcus furiosus* have been solved so far (Bond *et al.*, 2001; Nishino *et al.*, 2001). We present here the preparation and characterization of crystals from another member of the Hjc family originating from *Archaeoglobus fulgidus*.

2. Experimental procedures

2.1. Expression and purification of Hjc

The *A. fulgidus* Hjc monomer encompasses 136 residues (MW 15.4 kDa; theoretical pI 9.2). Its gene was amplified from genomic DNA (Neef *et al.*, 2002) and subcloned into the pET24 plasmid. The plasmid was transformed into *Escherichia coli* strain BL21 (DE3) Codon Plus RIL (Stratagene) which contains a plasmid carrying extra tRNA genes. The cells were grown at 310 K in 6 l LB medium containing 100 µg ml⁻¹ ampicillin and 87 µg ml⁻¹ chloramphenicol to an OD₆₀₀ of 0.8. After induction with 1 mM isopropyl thiogalactoside (IPTG, final concentration) cells were grown for another 2 h. They were harvested by centrifugation, resuspended in 50 ml lysis buffer [50 mM Tris-HCl pH 8, 0.1 M EDTA, 10% (w/v) glycerol, 0.4 M (NH₄)₂SO₄] and disrupted with a French press. The lysate was cleared



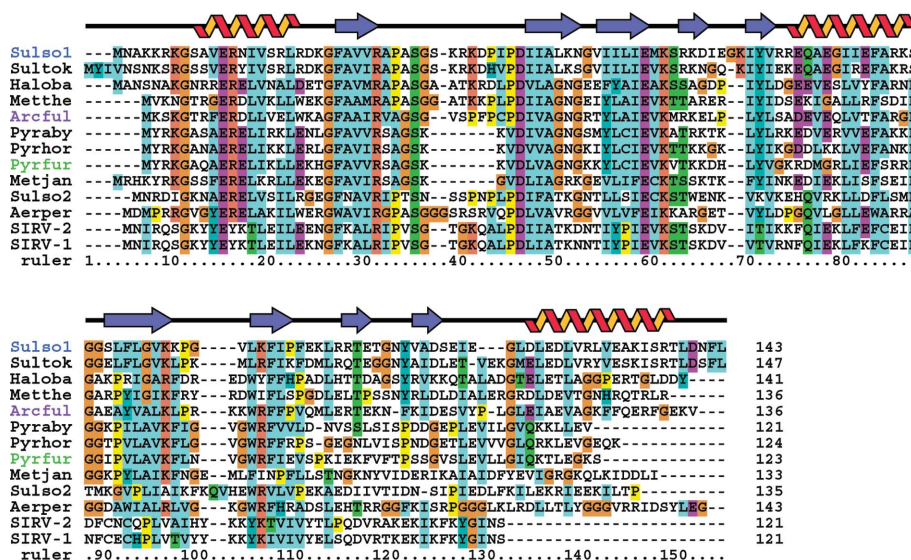


Figure 1 Sequence alignment of Hjc from different organisms: *Sulfolobus solfataricus*, *S. tokodaii*, *Halobacterium halobium*, *Methanobacterium thermoautotrophicum*, *Archaeoglobus fulgidus*, *Pyrococcus abyssi*, *P. horikoshii*, *P. furiosus*, *Methanococcus janaschii*, *Aeropyrum pernix* and SIRV (*S. islandicus*-infecting retrovirus). Secondary-structure elements present in the structure of the *S. solfataricus* monomer are indicated. The figure was prepared using CLUSTALW (Thompson *et al.*, 1994).

by centrifugation at 30 000g for 30 min after the addition of 10 ml lysis buffer. The supernatant was diluted ten times with buffer containing 50 mM Tris-HCl pH 8, 50 mM NaCl, 10% (w/v) glycerol, applied onto a 10 ml Heparin column (Amersham Biosciences) and eluted with a 0.1–1 M NaCl gradient. Fractions at about 0.75 M NaCl containing >90% Hjc were immediately applied onto a 5 ml hydroxyapatite column (BioRad Laboratories) and eluted with a 0.1–1 M sodium phosphate gradient at pH 7. The Hjc sample was further purified on a Superose 12 column (Amersham Biosciences) in 50 mM Tris-HCl pH 7, 0.4 M (NH₄)₂SO₄ (Fig. 2). Finally, the sample was concentrated by ultrafiltration in the same buffer to 10 mg ml⁻¹, stored at 278 K and used for crystallization assays.

2.2. Crystallization of Hjc

Crystallization experiments were carried out at 293 K. Initial conditions were determined using Wizard I and II sparse matrices (deCODE Genetics). Sitting drops of 2 µl (1:1 mixture of protein and screen solutions) were equilibrated by vapour diffusion against a reservoir containing 100 µl screen solution in Crystal Quick plates (Greiner Bio-One). Since crystals obtained in the screens (Table 1) were scarcely reproducible, we used counter-diffusion for further optimization. This method allows a self-screening of supersaturation and a self-refinement of growth conditions along the crystallization chamber, typically an X-ray capillary (López-Jaramillo *et al.*, 2001). Hjc sample solutions (6 µl) including 0.3% (w/v) low-gelling-point agarose (Serva) were introduced into 0.3 mm X-ray capillaries (Hampton Research). The gellified medium containing the protein was brought into contact with the crystallization solution at the wide end of the capillary as described previously (López-Jaramillo *et al.*, 2001; Biertümpfel *et al.*, 2002; Ng *et al.*, 2003).

2.3. Crystallographic characterization

Crystals obtained by vapour diffusion were mounted in cryoloops (Hampton Research), plunged into paraffin oil, flash-cooled in liquid propane and analyzed at 100 K. Crystals grown by counter-diffusion were gently blown out of the capillary, dissected from the agarose gel and frozen as described above.

Preliminary crystal characterization was performed on the in-house X-ray source (Enraf-Nonius FR 751 rotating-anode generator, total reflection double-focusing mirrors, MAR 345 IP detector). A first data set was collected on beamline ID14-EH1 (ESRF, France) using an ADSC Quantum 4 CCD detector from a frozen prismatic crystal, with a high-resolution pass (251 images of 0.3–0.5°, crystal-to-detector distance of 275 mm) and a low-resolution pass (45 images of 2° at 400 mm).

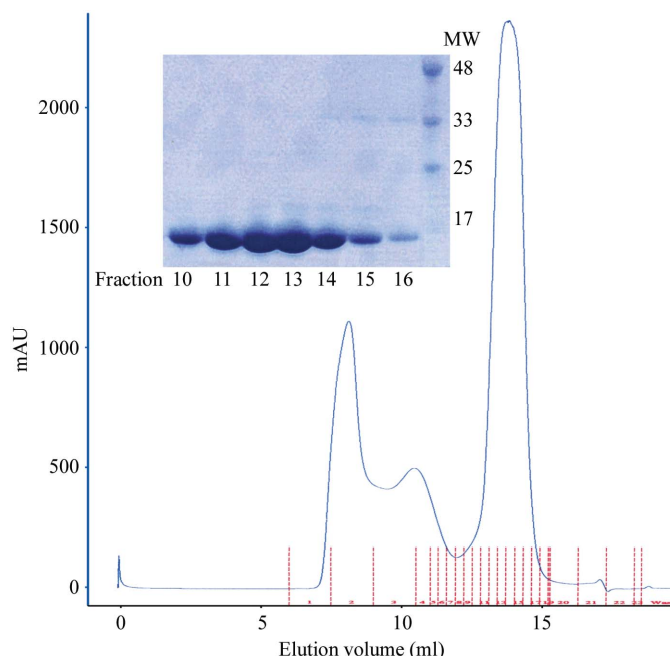


Figure 2 Last step of the purification of *A. fulgidus* Hjc. The chromatogram from gel filtration on a Superose 12 column shows the absorption at 280 nm as a function of elution volume. Peak fractions were collected (indicated in red) and checked by denaturing gel electrophoresis (insert). Fractions 10–14 were pooled as the Coomassie blue-stained gel shows that those samples yielded pure Hjc. The last lane contains molecular-weight markers.

Table 1

Screen solutions (from Wizard I and II) leading to Hjc crystallization.

	Crystallizing agent	Buffer	Salt	Crystal habit (size)
WI-01	20% (w/v) PEG 8000	100 mM CHES pH 9.5	—	Plate-like (200 µm)
WI-12	20% (w/v) PEG 1000	100 mM imidazole pH 8.0	200 mM Ca(OAc) ₂	Prism (<50 µm)
WI-21	20% (w/v) PEG 8000	100 mM HEPES pH 7.5	—	Plate-like (<50 µm)
WI-27	1.2 M/0.8 M NaH ₂ PO ₄ / K ₂ HPO ₄	100 mM CAPS pH 10.5	200 mM Li ₂ SO ₄	Plate-like (<50 µm)
WI-41	30% (w/v) PEG 3000	100 mM CHES pH 9.5	—	Prism (100 µm)
WII-34	10% (w/v) PEG 8000	100 mM imidazole pH 8.0	—	Plate-like (100 µm)

A second data set was measured on beamline X06SA (SLS, Switzerland) using a MAR CCD detector with a high-resolution pass (340 frames of 0.3° at 190 mm) and a low-resolution pass (101 frames of 1° at 400 mm). In this experiment, a plate-like crystal was mounted in a cryoloop and oriented with its (001) faces parallel to the incident beam using an arc appended to the goniometric head (90° goniometer head arc, Hampton Research). Data were processed using the *HKL* package (Otwinowski & Minor, 1997).

3. Results

The expression of Hjc in *E. coli* yielded about 20 mg protein from 6 l culture. The sample was >98% pure as judged from Coomassie blue-stained gel (Fig. 2).

Initial crystallization conditions were defined using sparse matrices. Hits were mainly obtained in PEG-containing solutions (Table 1) and yielded crystals of either prismatic or plate-like habit (Fig. 3). It turned out later that these conditions were scarcely reproducible using the initial technique (vapour diffusion).

Preliminary diffraction assays performed on the largest crystals obtained in the screen (conditions WI-01, WI-41, WII-34) indicated that both prismatic and plate-like forms had the same elongated trigonal unit cell. An initial data set was collected on a prismatic crystal (unit-cell parameters $a = b = 37.1$, $c = 270.2$ Å, $\gamma = 120^\circ$). Although these prisms did diffract beyond 2.5 Å at the ESRF, their random orientation in the cryoloop resulted in a high number of

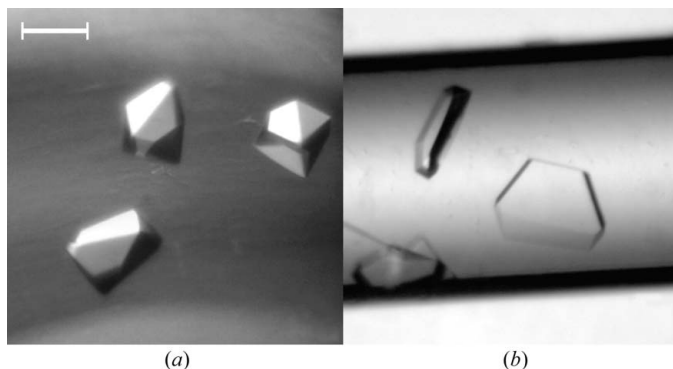


Figure 3

Different crystal habits of *A. fulgidus* Hjc resolvase. (a) Prismatic crystals obtained by sparse-matrix screening (condition WI-41) in sitting-drop vapour-diffusion experiments. (b) Plate-like crystals grown by counter-diffusion in a 0.3 mm thick X-ray capillary using 30% PEG 1000, 100 mM HEPES pH 7.5, 10 mM CaCl₂ and 0.3% (w/v) low-gelling agarose. Their large pseudo-hexagonal faces have indices (001) and are perpendicular to the crystallographic *c* axis. Both images are shown at the same magnification (scale bar = 100 µm).

Table 2

Data-collection statistics for Hjc plate-like crystals.

Values in parentheses are for the highest resolution shell.	
Synchrotron-radiation beamline	X06SA
Wavelength (Å)	0.980
Space group	<i>P</i> ₃ 21 or <i>P</i> ₃ 21
Unit-cell parameters (Å, °)	$a = b = 37.4$, $c = 271.8$, $\alpha = \beta = 90$, $\gamma = 120$
Mosaicity (°)	0.47
Resolution (Å)	60–2.7
Observed reflections	38974
Unique reflections	6708
Redundancy	5.8
R_{sym}^\dagger (%)	6.4 (19.7)
$\langle I \rangle / \langle \sigma(I) \rangle$	20.3 (4.5)
Completeness (%)	98.9 (94.6)

$$\dagger R_{\text{sym}} = \frac{\sum_{hkl} \sum_i |I_i(hkl) - \langle I(hkl) \rangle|}{\sum_{hkl} \sum_i I_i(hkl)}$$

reflection overlaps in the c^* direction and a poor completeness at high resolution (84% overall, 70% in the highest shell).

Since prismatic crystals were difficult to grow and to orient for optimal data collection owing to their isometric shape, plate-like crystals were chosen for further investigation. Their tendency to lie in the plane of cryoloops made positioning of the *c* axis (see Fig. 3) with respect to the X-ray beam much easier. These crystals were prepared by counter-diffusion in agarose gel. After adjusting the crystallization mix (buffer, salt and PEG), they reached a size of 0.15 mm after two weeks (Fig. 3b). This strategy had two important advantages. Firstly, it increased the reproducibility of crystallization, benefitting from the wide supersaturation range screened in each assay. Secondly, the fragile Hjc plates were protected by the agarose gel and adhered easily to cryoloops. This facilitated their handling and their soaking in paraffin oil. Indeed, the whole cryocooling procedure was enhanced using these gel-grown crystals.

Once frozen, one of these crystals was mounted in the X-ray beam using an arc appended to the goniometer head. It was analyzed at beamline X06SA (SLS, Switzerland) and showed a unit cell similar to that of prismatic crystals. However, reflection overlaps could be avoided by orienting the (001) faces of Hjc plates parallel to the incident beam and thereby aligning the *c* axis along the oscillation axis. A complete data set was collected at 2.7 Å resolution. Data-collection statistics are given in Table 2. The data belong to point group 32 and systematic absences of (00 l) reflections (Fig. 4) account for space group *P*₃21 or *P*₃21. No indications of twinning were detected (Yeates, 1997).

The known Hjc structures (PDB codes 1gef, 1ipi and 1hh1; Nishino *et al.*, 2001; Bond *et al.*, 2001) were used to derive input models for molecular replacement (MR). Polyalanine and full-sequence models were generated with *MODELLER* (Sali & Blundell, 1993). The self-rotation function analysis suggests the presence of a non-crystallographic twofold axis (Fig. 4b). This situation would lead to a dimer in the asymmetric unit (AU) and a low solvent content of 31% ($V_M = 1.78$ Å³ Da⁻¹) compared with 65% ($V_M = 3.51$ Å³ Da⁻¹) for the case of one monomer per AU. Both monomeric and dimeric models were tried with the programs *AMoRe* (Navaza, 1994), *CNS* (Brünger *et al.*, 1998) and *EPMR* (Kissinger *et al.*, 1999), but all attempts failed. Similar difficulties with MR have recently been reported for the closely related Holliday junction endonuclease (Hje) from *S. solfataricus* (Middleton *et al.*, 2003) and for SIRV2 Hjc (Ennifar *et al.*, 2005). This is probably a consequence of the sequence variability and the architectural flexibility of these dimeric enzymes (Middleton *et al.*, 2004).

In conclusion, the reproducibility of *A. fulgidus* Hjc crystallization was improved by employing the counter-diffusion method. Moreover,

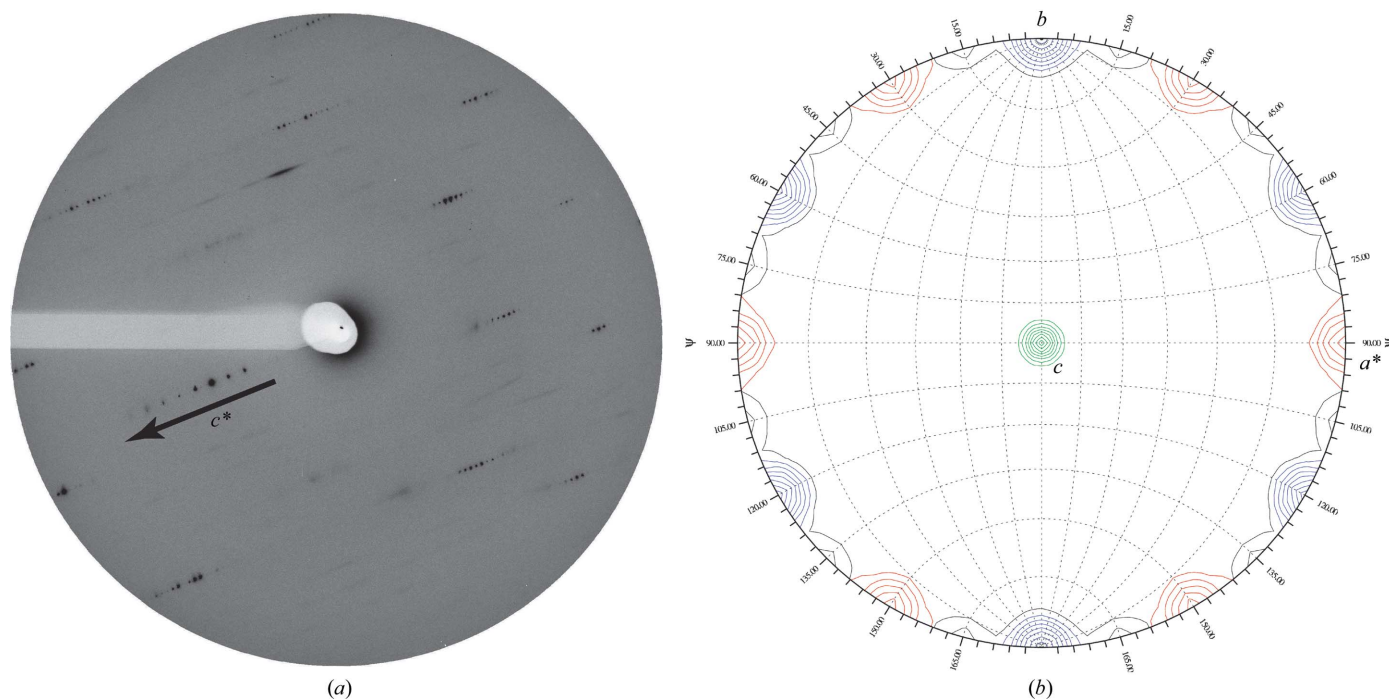


Figure 4 Analysis of Hjc plate-like crystals. (a) Diffraction pattern from a crystal oriented with its c axis along the oscillation axis in order to ensure the best reflection separation in the c^* direction. Extinctions of the $(00l)$ reflections are characteristic of a threefold screw axis. This image from a low-resolution pass (5 Å at the edge of the MAR CCD detector) corresponds to a single rotation of 1.5° at a distance of 400 mm. (b) Stereographic representation of the self-rotation function at $\kappa = 180^\circ$ and $\kappa = 120^\circ$ generated by *GLRF* (Tong & Rossmann, 1990, 1997) with a resolution range of 12–4 Å and an integration radius of 28 Å. Peaks corresponding to twofold and threefold crystallographic symmetry (blue, $\kappa = 180^\circ$ and green, $\kappa = 120^\circ$, respectively) are normalized at a value of 1000. The observation of non-crystallographic twofold axes (red, $\kappa = 180^\circ$; peak level of ~ 700) suggests the presence of a Hjc dimer in the asymmetric unit.

this preliminary analysis of Hjc crystals shows that the drawback of a long unit-cell parameter can be overcome by using properly oriented plate-like crystals. In order to circumvent difficulties with MR, structure determination using alternative phasing strategies is in progress.

The authors are grateful for beamtime allocation and appreciate the assistance of E. Mitchell and colleagues at ID14 beamlines (ESRF, France), and C. Schulze-Briese and T. Tomizaki at beamline X06SA (SLS, Switzerland) during data collection. CS was the recipient of a Marie Curie Individual Fellowship (IHP Programme, contract No. HPMF-2000-00434) and CB was the recipient of a fellowship from the International PhD Programme of the European Molecular Biology Laboratory. This work was partly supported by the Deutsche Forschungsgemeinschaft (DFG Normalverfahren SU61/6-2).

References

- Biertümpfel, C., Basquin, J., Suck, D. & Sauter, C. (2002). *Acta Cryst.* **D58**, 1657–1659.
- Bond, C., Kvaratskhelia, M., Richard, D., White, M. & Hunter, W. (2001). *Proc. Natl Acad. Sci. USA*, **98**, 5509–5514.
- Brünger, A. T., Adams, P. D., Clore, G. M., DeLano, W. L., Gros, P., Grosse-Kunstleve, R. W., Jiang, J.-S., Kuszewski, J., Nilges, M., Pannu, N. S., Read, R. J., Rice, L. M., Simonson, T. & Warren, G. L. (1998). *Acta Cryst.* **D54**, 905–921.
- Daiyasu, H., Komori, K., Sakae, S., Ishino, Y. & Toh, H. (2000). *Nucleic Acids Res.* **28**, 4540–4543.
- Ennifar, E., Basquin, J., Birkenbihl, R. & Suck, D. (2005). *Acta Cryst.* **F61**, 507–509.
- Holliday, R. (1964). *Genet. Res.* **5**, 282–304.
- Kissinger, C., Gehlhaar, D. & Fogel, D. (1999). *Acta Cryst.* **D55**, 484–491.
- Komori, K., Sakae, S., Shinagawa, H., Morikawa, K. & Ishino, Y. (1999). *Proc. Natl Acad. Sci. USA*, **96**, 8873–8878.
- Kvaratskhelia, M., Wardleworth, B., Norman, D. & White, M. (2000). *J. Biol. Chem.* **275**, 25540–25546.
- Lilley, D. & White, M. (2001). *Nature Rev. Mol. Cell Biol.* **2**, 433–443.
- López-Jaramillo, F. J., García-Ruiz, J. M., Gavira, J. A. & Otálora, F. (2001). *J. Appl. Cryst.* **34**, 365–370.
- Middleton, C. L., Parker, J. L., Richard, D. J., White, M. F. & Bond, C. S. (2003). *Acta Cryst.* **D59**, 171–173.
- Middleton, C. L., Parker, J. L., Richard, D. J., White, M. F. & Bond, C. S. (2004). *Nucleic Acids Res.* **32**, 5442–5451.
- Navaza, J. (1994). *Acta Cryst.* **A50**, 157–163.
- Neef, K., Birkenbihl, R. P. & Kemper, B. (2002). *Extremophiles*, **6**, 359–367.
- Ng, J. D., Gavira, J. A. & García-Ruiz, J. M. (2003). *J. Struct. Biol.* **142**, 218–231.
- Nishino, T., Komori, K., Tsuchiya, D., Ishino, Y. & Morikawa, K. (2001). *Structure*, **9**, 197–204.
- Otwinowski, Z. & Minor, W. (1997). *Methods Enzymol.* **276**, 307–326.
- Sali, A. & Blundell, T. (1993). *J. Mol. Biol.* **234**, 779–815.
- Sharples, G. (2001). *Mol. Microbiol.* **39**, 823–834.
- Thompson, J., Higgins, D. & Gibson, T. (1994). *Nucleic Acids Res.* **22**, 4673–4680.
- Tong, L. & Rossmann, M. G. (1990). *Acta Cryst.* **A46**, 783–792.
- Tong, L. & Rossmann, M. G. (1997). *Methods Enzymol.* **276**, 594–611.
- White, M., Giraud-Panis, M., Pöhler, J. & Lilley, D. (1997). *J. Mol. Biol.* **269**, 647–664.
- Yeates, T. O. (1997). *Methods Enzymol.* **276**, 344–358.